Electronic Supplementary Material (ESI) for Journal of Materials Chemistry A.

Supporting information for

Oxygenated P/N co-doped carbon for efficient 2e$^-$ oxygen reduction to H_2O_2

Zongge Li [a,b], Anuj Kumar[d], Nianxi Liu [a], Ming Cheng [b], Changkai Zhao [a], Xiangshe Meng [a], Huifang Li [c], Ying Zhang [b], Zhiming Liu [c], Guoxin Zhang *[a], and Xiaoming Sun [e]

a. Department of Energy Storage Technology, Shandong University of Science and Technology, Qingdao 266590, Shandong, China.

b. State Key Laboratory of Heavy Oil Processing, China University of Petroleum (East China), Qingdao 266580, Shandong, China.

c. College of Electromechanical Engineering, Shandong Engineering Laboratory for Preparation and Application of High-performance Carbon-Materials, Qingdao University of Science & Technology, Qingdao 266061, Shandong, China.

d. Department of Chemistry, GLA University, Mathura 281406, India.

e. State Key Laboratory of Chemical Resource Engineering, Beijing Advanced Innovation Center for Soft Matter Science and Engineering, College of Chemistry, Beijing University of Chemical Technology, Beijing 100029, China.

* Corresponding authors. zhanggx@sdust.edu.cn (Guoxin Zhang)

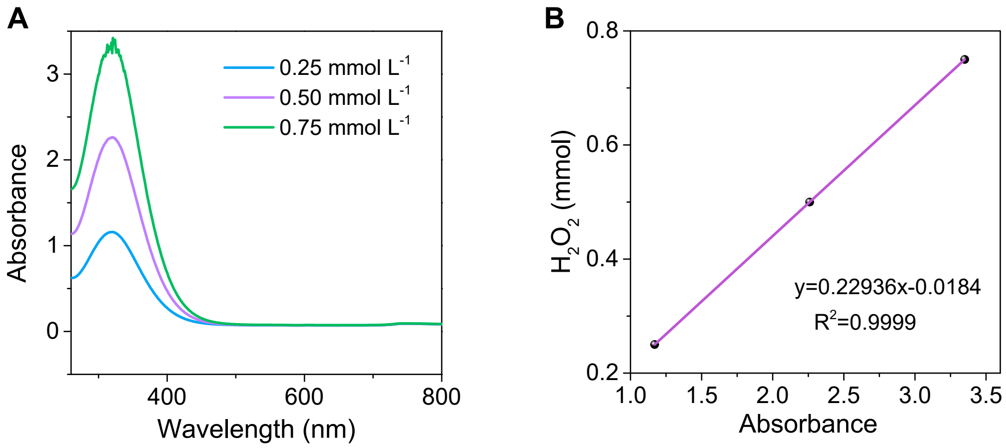

Figure S1. (A) UV-vis spectra of $Ce(SO_4)_2$ solution of different concentrations. (B) The standard curve of $Ce(SO_4)_2$ titration method

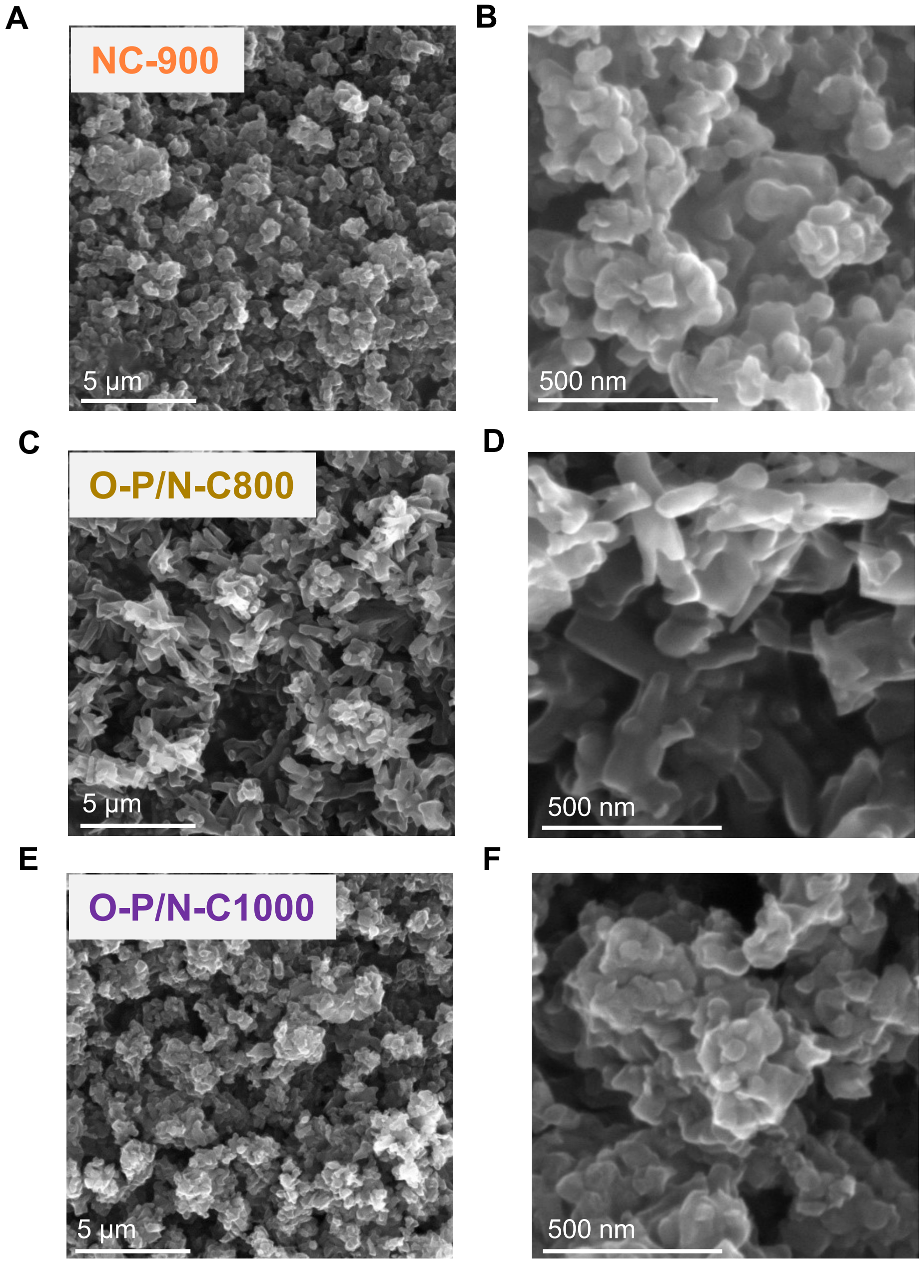

Figure S2. SEM images of (A-B) NC-900, (C-D) O-P/N-C800 and (E-F) O-P/N-C1000.

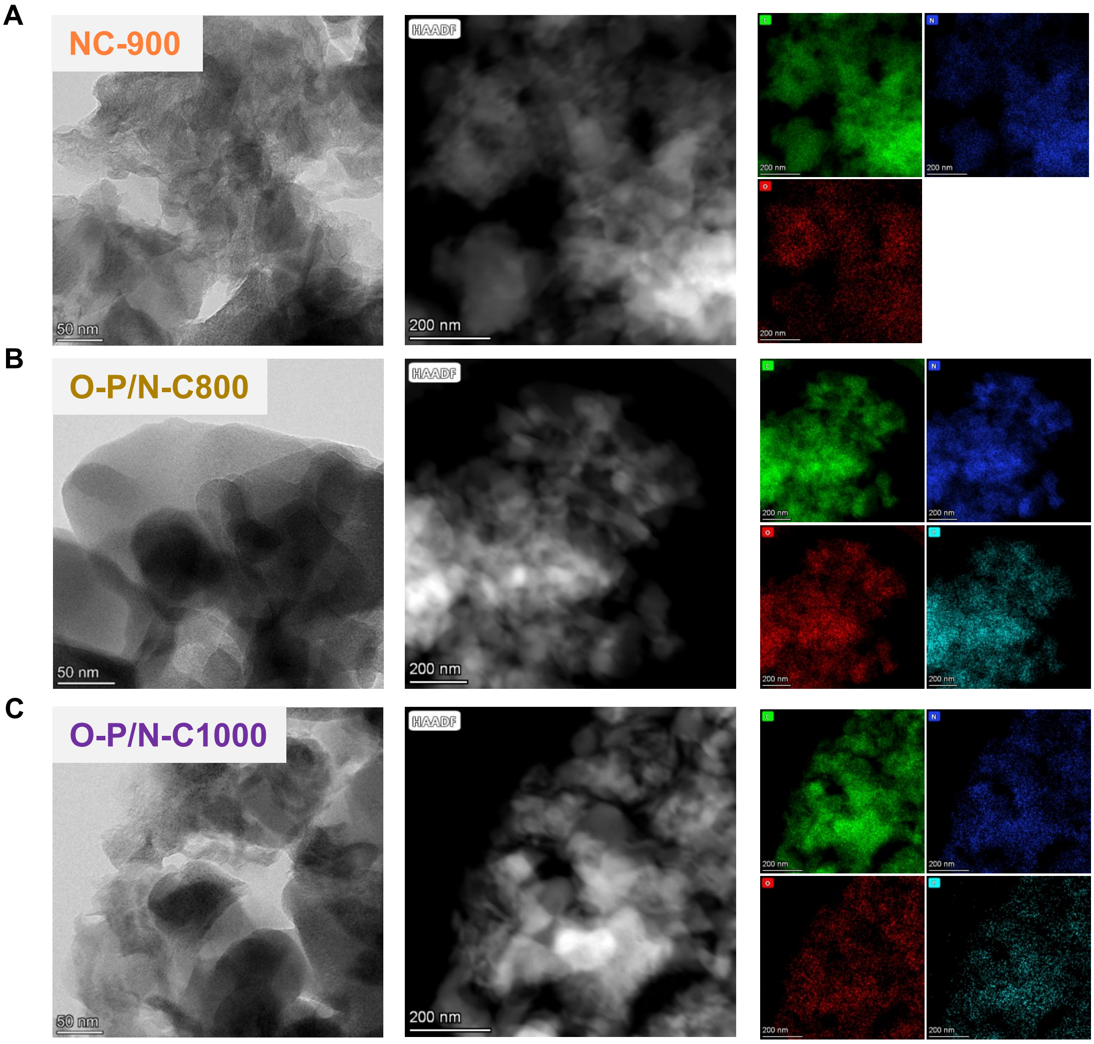

Figure S3. TEM images and HAADF-HRTEM EDS of (A) NC-900, (B) O-P/N-C800 and (C) O-P/N-C1000.

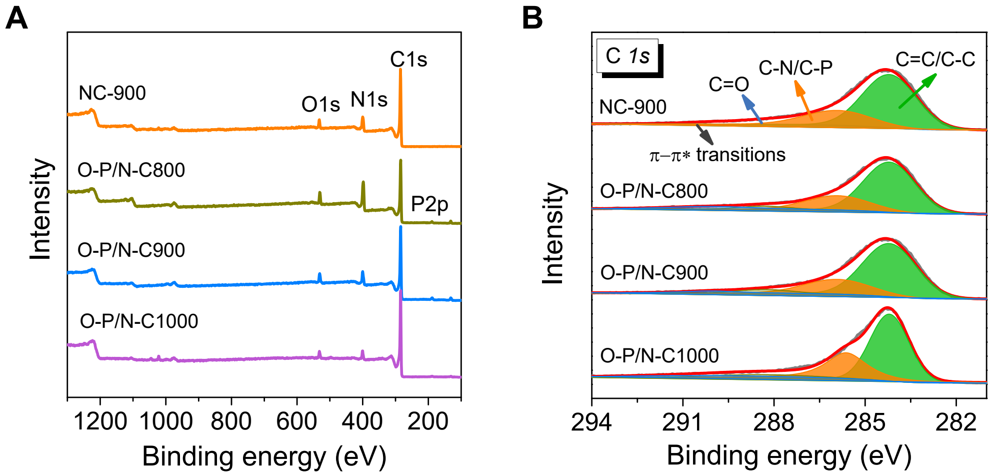

Figure S4. (A) XPS element survey, (B) C 1s spectra of NC-900, O-P/N-C800, O-P/N-C900 and O-P/N-C1000.

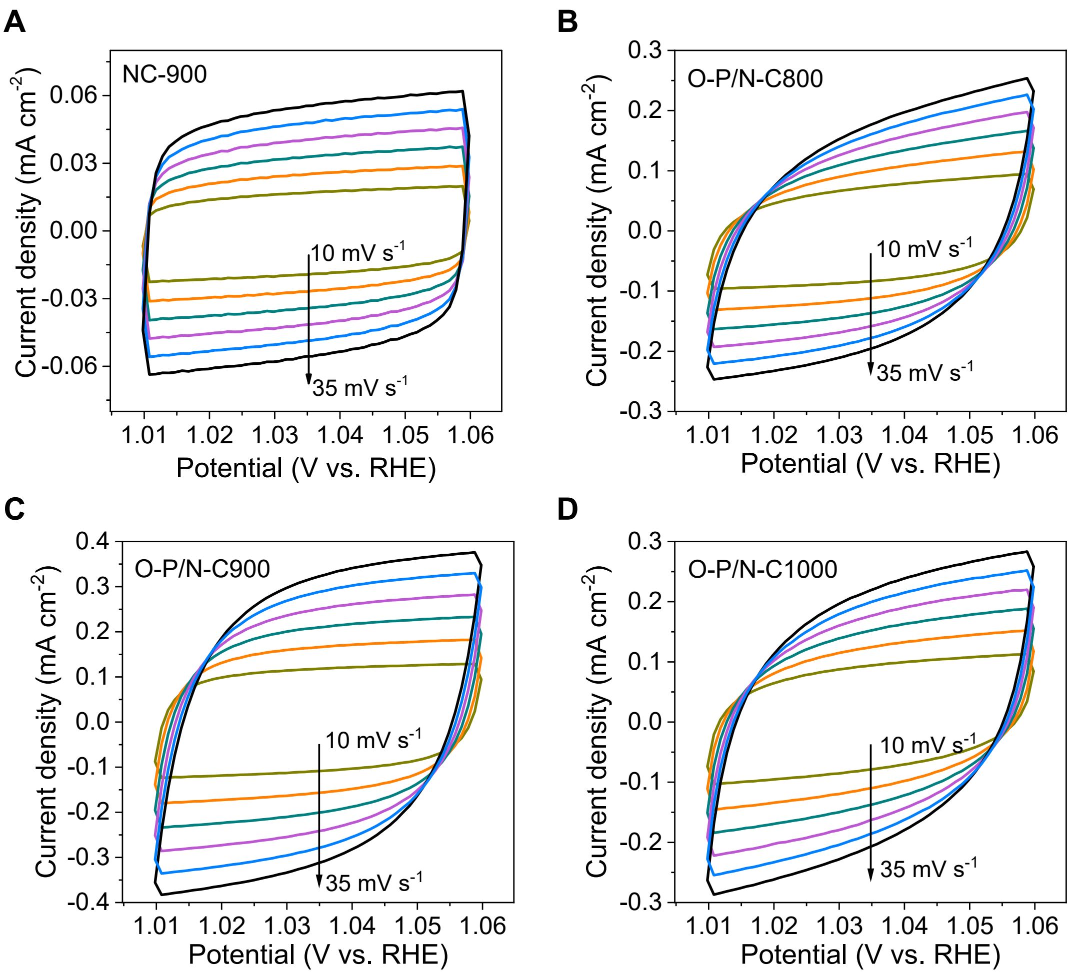

Figure S5. CV curves of (A) NC-900, (B) O-P/N-C800, (C) O-P/N-C900 and (D) O-P/N-C1000 at different scan rates in the potential range of 1.01-1.06 V (vs. RHE).

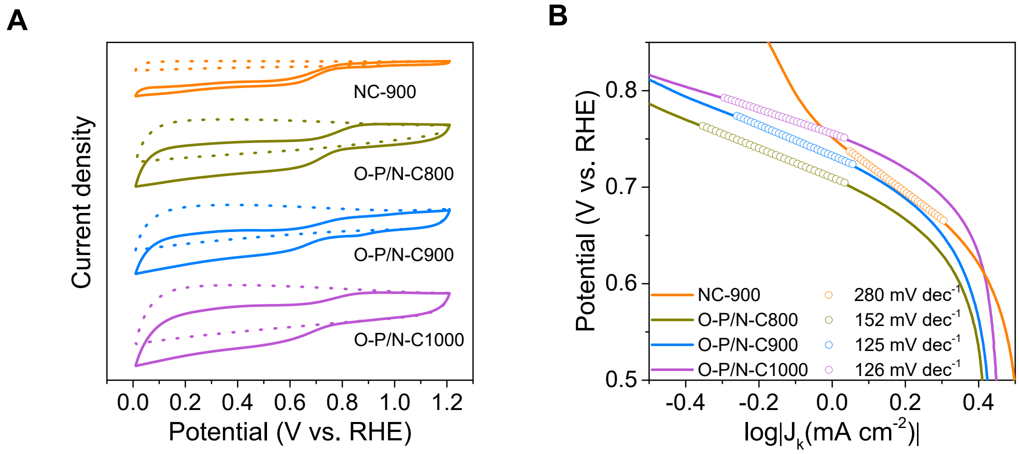

Figure S6. (A) CV curves (The dotted and solid lines represent N_2- and O_2-saturated electrolytes, respectively), and (B) Tafel slops of NC-900, O-P/N-C800, O-P/N-C900 and O-P/N-C1000.

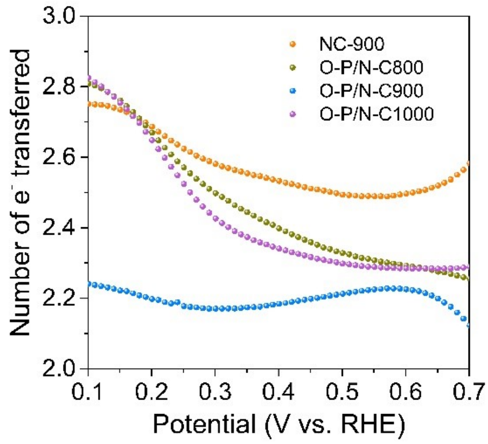

Figure S7. Calculated curves of transfer electron number (n) of NC-900, O-P/N-C800, O-P/N-C900 and O-P/N-C1000 samples.

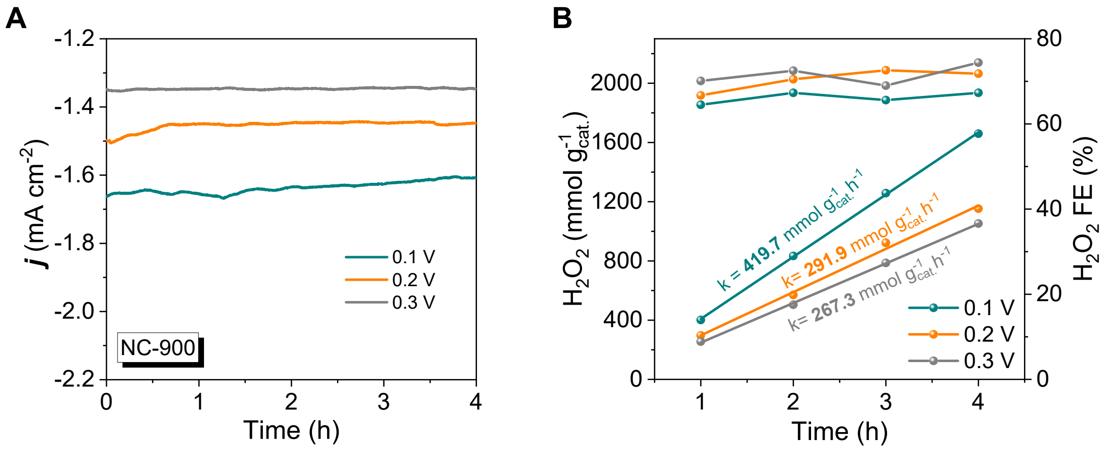

Figure S8. (A) Current stability and (B) H_2O_2 production rate and faradaic efficiency (FE, %) of O-P/N-C900 at 0.1, 0.2, and 0.3 V (vs. RHE) with the catalyst loading amount of 1 mg cm^{-2}.

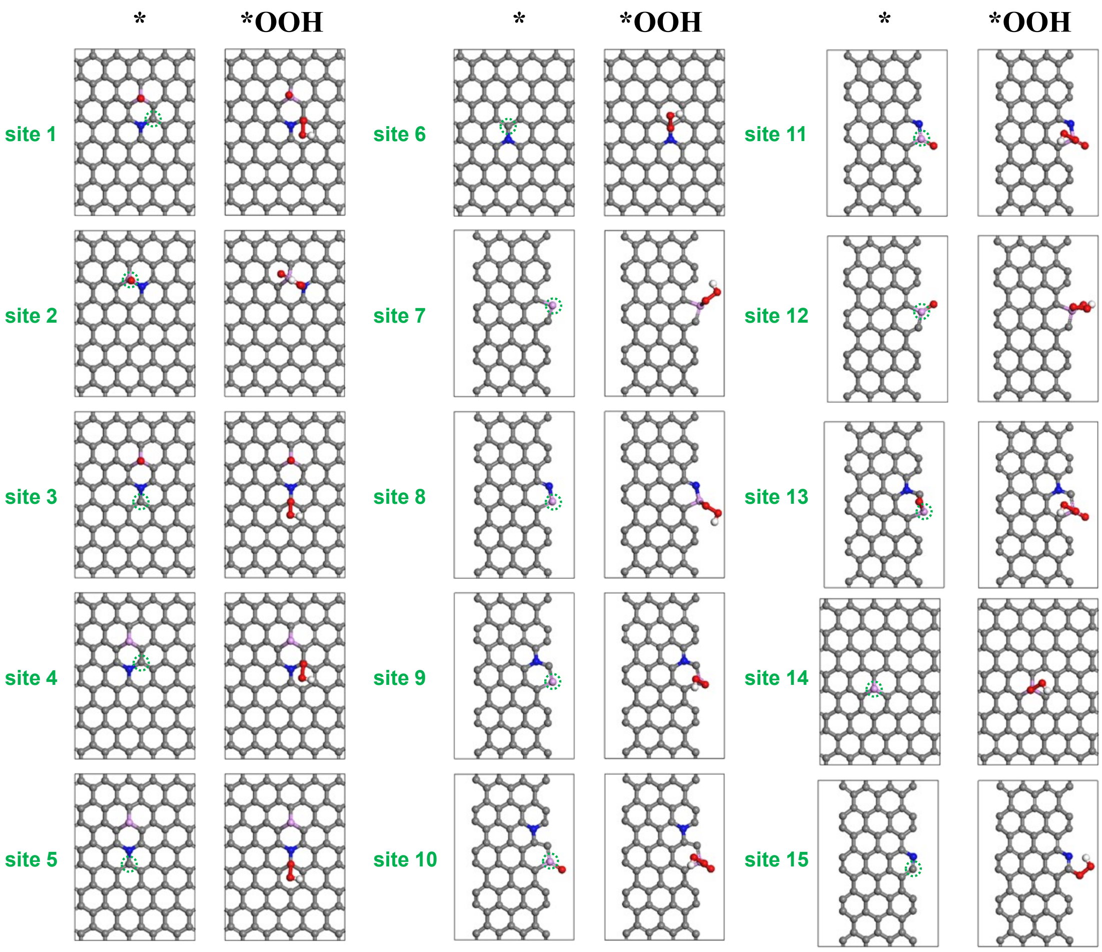

Figure S9. The atomic structures of the examined oxygen functional groups. Color code: carbon, gray; oxygen, red; hydrogen, white; nitrogen, blue; phosphorus, pink. The corresponding examined active sites are marked with a dashed green circle in each model structure.

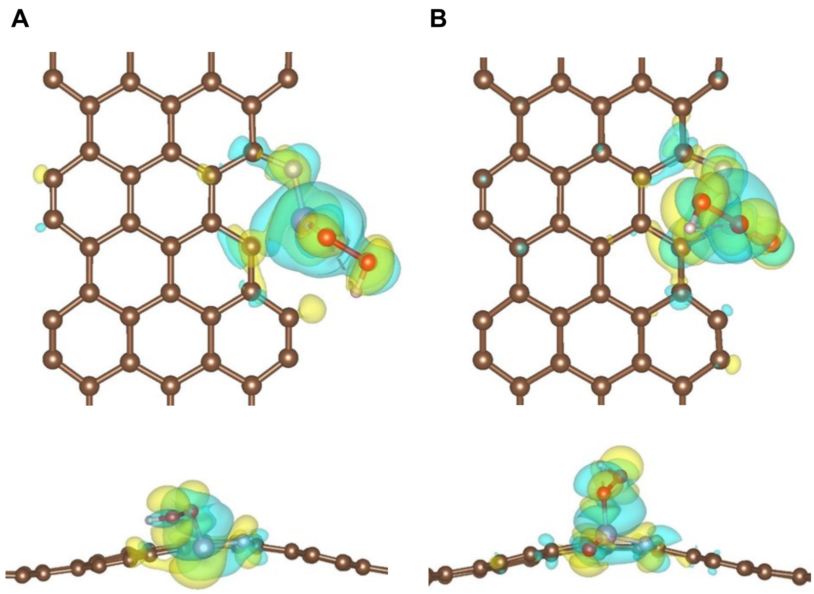

Figure S10. Differential charge distribution of (A) site 8 (edged N-P) and (B) site 11 (edged N-P=O) after absorbing OOH species.

Table S1. XPS element contents of NC-900 and O-P/N-C samples.

Sample	C	N	O	P
NC-900	81.44	13.59	4.97	——
O-P/N-C800	68.19	23.87	6.18	1.76
O-P/N-C900	80.74	11.56	5.21	2.49
O-P/N-C1000	88.46	6.92	3.99	0.63

Table S2. Comparison of H_2O_2 production on various electrocatalysts in H-type cells.

Catalyst	Electrolyte	Production rate	Reference
Oxo-G/NH_3	0.1 M KOH	224.8 mmol g^{-1} h^{-1}	1
Co-SAs NC	0.1 M KOH	38.1 mmol g^{-1} h^{-1}	2
BNTO	1 M KOH	208 mmol g^{-1} h^{-1}	3
CNO-glu-H	0.1 M KOH	200 mmol g^{-1} h^{-1}	4
DGLC	0.1 M KOH	355 mmol g^{-1} h^{-1}	5
Fe_2O_{3-x}	0.1 M KOH	454 mmol g^{-1} h^{-1}	6
NCMK3IL50	0.1 M KOH	561.7 mmol g^{-1} h^{-1}	7
Ni-MOF NS	0.1 M KOH	80 mmol g^{-1} h^{-1}	8
Ni-NPs BC	0.1 M KOH	162.7 mmol g^{-1} h^{-1}	9
NOC-6M	0.1 M KOH	548.8 mmol g^{-1} h^{-1}	10

SA ZnO_3C	0.1 M KOH	350 mmol g^{-1} h^{-1}	11
O-P/N-C900	**0.1 M KOH**	**698.4 mmol g^{-1} h^{-1}**	**This work**

References

1. L. Han, Y. Sun, S. Li, C. Cheng, C. E. Halbig, P. Feicht, J. L. Hübner, P. Strasser and S. Eigler, *ACS Catal.*, 2019, **9**, 1283-1288.
2. 54. H. Xu, S. Zhang, J. Geng, G. Wang and H. Zhang, *Inorg. Chem. Front.*, 2021, **8**, 2829-2834.
3. Z. Zhang, Q. Dong, P. Li, S. L. Fereja, J. Guo, Z. Fang, X. Zhang, K. Liu, Z. Chen and W. Chen, *J. Phys. Chem. C*, 2021, **125**, 24814-24822.
4. H. Shao, Q. Zhuang, H. Gao, Y. Wang, L. Ji, X. Wang, T. Zhang, L. Duan, J. Bai, Z. Niu and J. Liu, *Inorg. Chem. Front.*, 2021, **8**, 173-181.
5. C. Zhang, J. Zhang, J. Zhang, M. Song, X. Huang, W. Liu, M. Xiong, Y. Chen, S. Xia, H. Yang and D. Wang, *ACS Sustainable Chem. Eng.*, 2021, **9**, 9369-9375.
6. R. Gao, L. Pan, Z. Li, C. Shi, Y. Yao, X. Zhang and J. J. Zou, *Adv. Funct. Mater.*, 2020, **30**, 1910539.
7. Y. Sun, I. Sinev, W. Ju, A. Bergmann, S. Dresp, S. Kühl, C. Spöri, H. Schmies, H. Wang, D. Bernsmeier, B. Paul, R. Schmack, R. Kraehnert, B. Roldan Cuenya and P. Strasser, *ACS Catal.*, 2018, **8**, 2844-2856.
8. M. Wang, X. Dong, Z. Meng, Z. Hu, Y. G. Lin, C. K. Peng, H. Wang, C. W. Pao, S. Ding, Y. Li, Q. Shao and X. Huang, *Angew. Chem., Int. Ed.*, 2021, **60**, 11190-11195.
9. H. Xu, M. Jin, J. Geng, S. Zhang and H. Zhang, *Sci. China Mater.*, 2021, **65**, 721-731.
10. C. Zhang, G. Liu, B. Ning, S. Qian, D. Zheng and L. Wang, *Int. J. Hydrogen Energy*, 2021, **46**, 14277-14287.
11. Y. Jia, Z. Xue, J. Yang, Q. Liu, J. Xian, Y. Zhong, Y. Sun, X. Zhang, Q. Liu, D. Yao and G. Li, *Angew. Chem., Int. Ed.*, 2022, **61**, 202110838.